Aeroelastic Tailoring for Flutter Constraints

by

J.Schweiger*, O.Sensburg**, C.Ponzi*

MESSERSCHMITT-BÖLKOW-BLOHM GMBH
Hubschrauber und Flugzeuge
P.O. Box 801160, 3 Munich 80
W.-Germany

Introduction

A horizontal stabilizer and control surface in front of the main wing offers several advantages over conventional tail-mounted surfaces:

- at take off the foreplane produces additional lift when the aircraft rotates, thus shortening the required runway length;
- in manoeuvres the aircraft can pull up immediately compared to the initial dive due to negative lift of the tailplane;
- foreplanes are more effective for active control, drag modulation, and
- they can easier be designed to be virtually spin-proof because a stalling foreplane will cause the aircraft to dive nose down before the wing begins to stall.

In this investigation, an aircraft similar to fig. 1 is considered to be naturally stable in supersonic flight and unstable at subsonic speeds, using active control technology (CCV). This leads to minimum induced drag at supersonic speeds.

If the canard actuation system should fail, the wing flaps only can be used for longitudinal control, and if the canard is free-floating (weathercock stability) no artificial stabilisation is necessary for the subsonic case. Since back-up stiffness is zero there is a great danger of flutter. So one main question of this investigation was: Is it possible to find a structural arrangement for the canard that allows flutter-free subsonic flight in a free-floating mode?

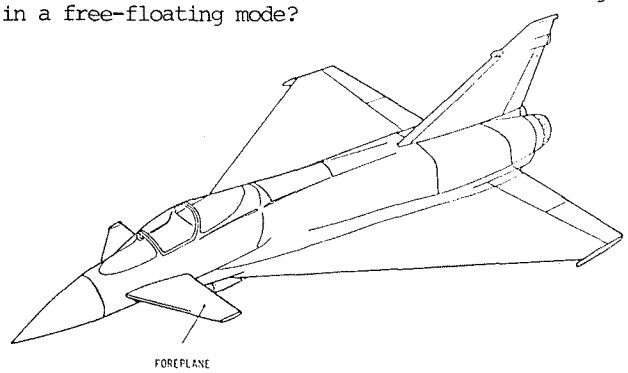

Fig. 1 Canard configuration

*) Aerospace Engineers
**) Head Structural Dynamics

A large amount of research was performed trying to find optimum CFC laminates - the so-called aeroelastic tailoring [1, 2] . This paper summarizes the major findings of a study described in [3] .

Theoretical Model

For this study, the program TSO [4] was used to analyse and optimize the static, dynamic, and aeroelastic behaviour of the canard. The program was modified by MBB and includes now a different optimisation-algorithm which allows to start with infeasible structures, and a supersonic Mach box method [5]. The structure of an aerodynamic surface is modelled as a trapezoidal plate.
This plate consists of an upper and lower part with up to three different layer orientations. The thicknesses of these layers are described with biquadratic polynominals in a swept, non-dimensional coordinate system of the plate. The airfoil thickness is simulated in the same way. The connection between upper and lower surface is considered to be rigid (no shear transfer). Fig. 2 shows the planform geometry, of the canard model, the structural box and the spigot attachment to the fuselage.

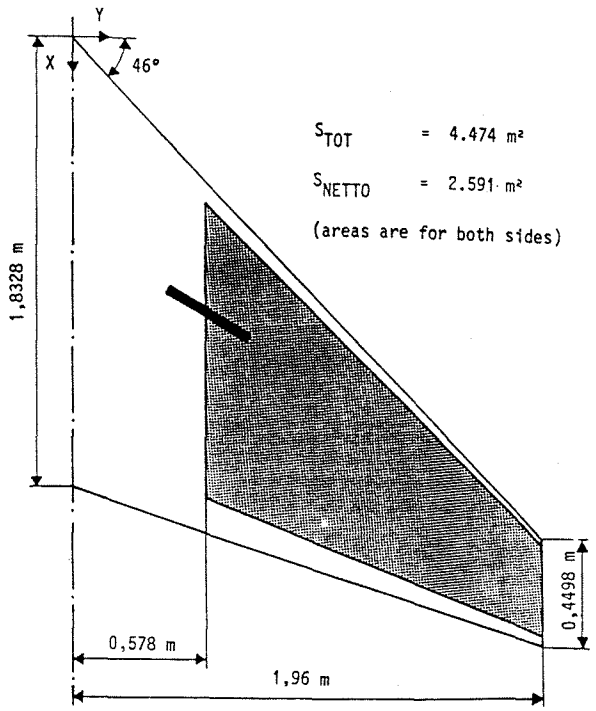

Fig. 2 Foreplane geometry and structural arrangement

For the dynamic analysis, additional masses (for the core, leading and trailing edges, and for non-structural items) are distributed as shown in fig.3.

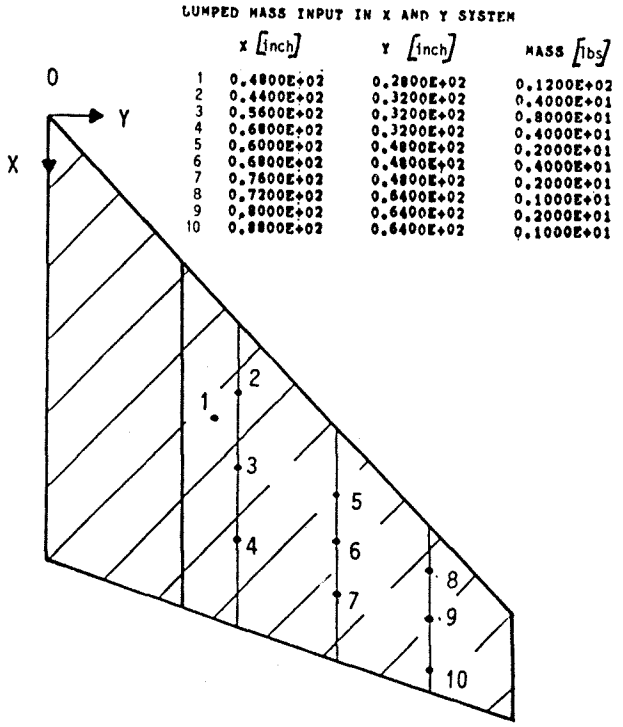

Fig. 3 Mass distribution

The idealisation of the steady and unsteady aerodynamic models are depicted in fig. 4.

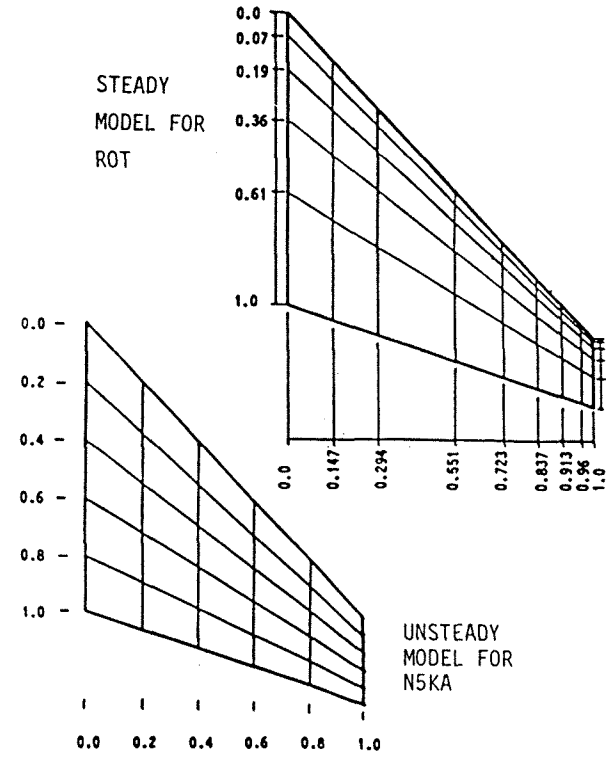

Fig. 4 Aerodynamic models

For the strength design of the cover skins three static load cases were used. These loads are single forces in different locations, fig. 5, the force is 68 kN for all cases.

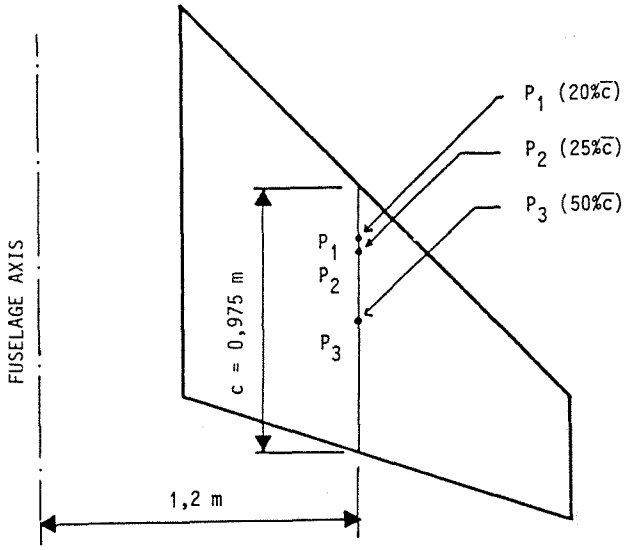

Fig. 5 Static load cases

In addition, TSO can calculate the proper load distribution fo a steady aeroelastic equilibrium condition. For this case the aerodynamic influence coefficient matrix for a given Mach number is calculated in a separate program and stored for TSO. For the discrete and dynamic pressure, the correct load distribution will then be obtained for the structural design. To simulate the attachment stiffness, two rotational stiffnesses for pitch and roll and a linear stiffness in z-direction were used (fig. 6).

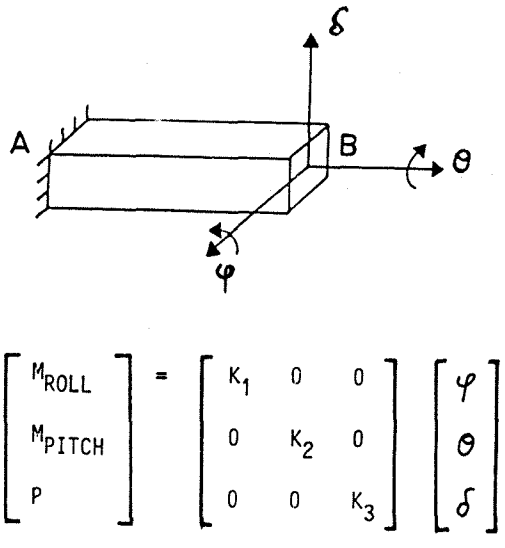

Fig. 6 Model for spigot attachment

The material properties and allowables are given in table 1.

E_{11}	= 130 000	N/mm²
E_{22}	= 5 850	N/mm²
ν_{12}	= 0,3	
G	= 3 000	N/mm²
ε_{11}	= 0.004	
ε_{22}	= 0.004	
ε_{12}	= 0.015	

TABLE 1 : MATERIAL PROPERTIES FOR UD-FIBERS

A difficulty with TSO can be that the program needs a feasible initial design to start with the optimization. Besides strength, minimum layer thickness (1ply) and maximum thickness (1/2 of profile depth) are permanent constraints. In this case, the small depth of the box along trailing edge and tip made it difficult to find an initial structure that meets strength requirements for all four load cases.

During this study, a new optimization algorithm (method of multipliers) was used. This 'Augmented-Lagrangian-Type' method can also handle infeasible designs, and it usually obtains better results from the optimization because the ill-conditioning of the inverse Hessian matrix during the optimization is avoided.

ANALYSIS

The program was applied in two steps:

1. Strength Design

The attachment stiffness coefficient for the strength designs have been chosen as:
$K_1 = 508 \frac{kNm}{rad}$, $K_2 = 734 \frac{kNm}{rad}$, and $K_3 = 175 \frac{kN}{m}$.

Fig. 7 depicts the layer composition and fiber orientations for a strength design with a symmetrical and balanced laminate. The deformations for the different load cases are shown in fig. 8. The dynamic modes and the flutter calculation for this case are depicted in fig. 9 and 10.

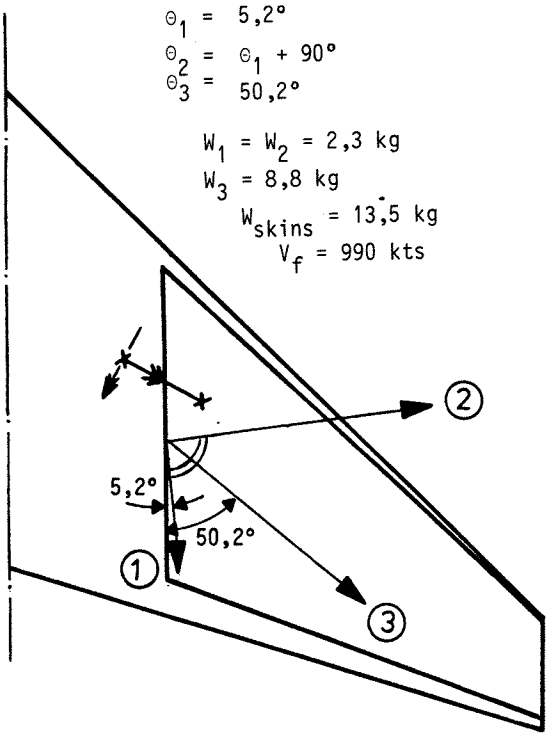

Fig. 7 Thickness distributions for strength design

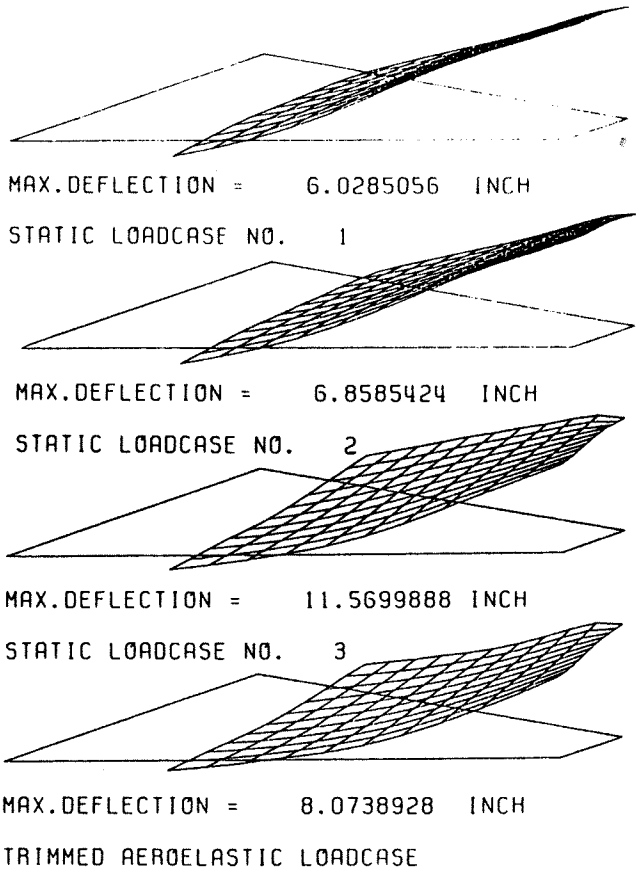

Fig. 8 Deformations for static load cases

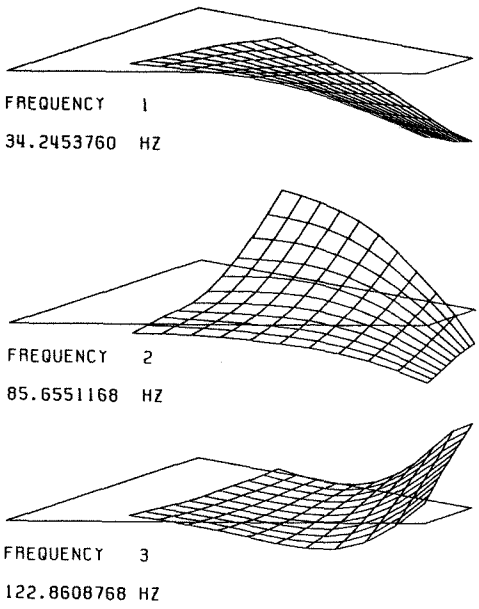

Fig. 9 Elastic mode shapes

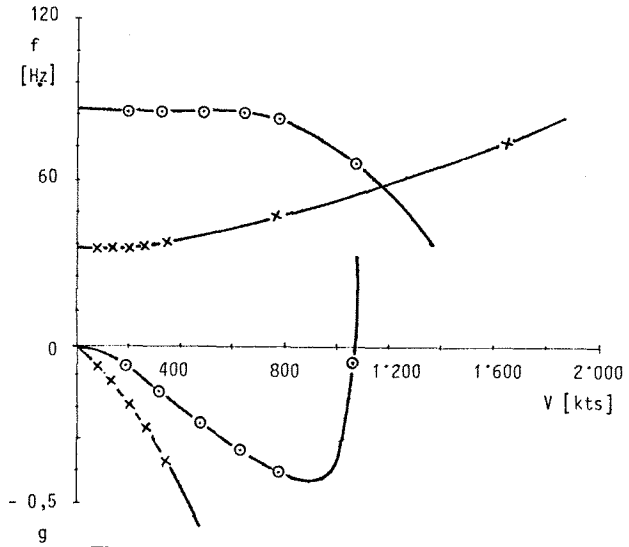

Fig. 10 Results of flutter calculation for strength design

2. Dynamic Analysis and Optimisation

Variation of Spigot Geometry

To study the dynamic system, the location of the spigot axis was varied for fixed stiffnesses of the skins and the spigot itself. First the sweep angle of the spigot axis was varied by rotating it about a fixed point at the mean aerodynamic chord for the forward center of pressure at x/c= 0.25. Fig. 11 indicates the change in flutter speed between 0 and 50 degrees sweep angle with an optimum at 30 degrees which was selected for the further studies.

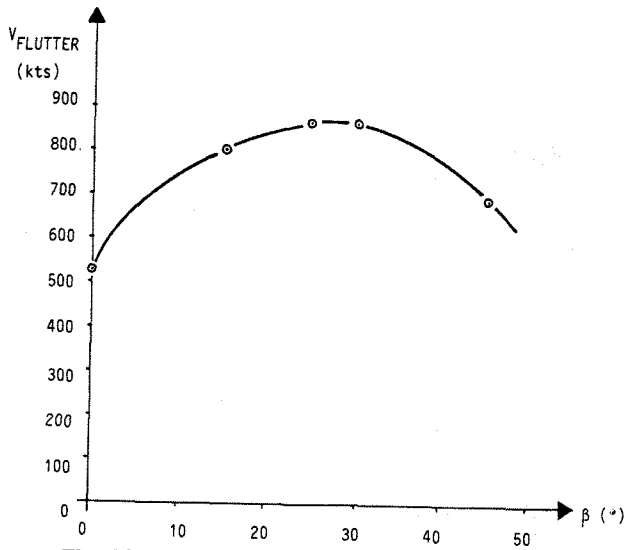

Fig. 11 Influence of spigot axis sweep angle on flutter speed

Type of Attachment

The dynamic behaviour of an aerodynamic surface can usually be analysed with the assumption of a clamped root because of several attachment points. But in the case of an all-movable surface, the single point attachment is decisive for the dynamic system. Also for infinite torsional stiffness of the spigot, the dynamic modes of the surface are very different from those of a fixed root model. Fig. 12 shows the first three eigenmodes for a typical design, using high stiffness values for the attachment.

The first mode (bending) is mainly defined by the structural design of the cover skins. The spigot roll stiffness is very high in general and does not affect this mode very much. The shape of mode no. 2 is given by the single point attachment, the frequency mainly by the spigot pitch stiffness. Efforts to change this mode by structural means have only a very limited potential.

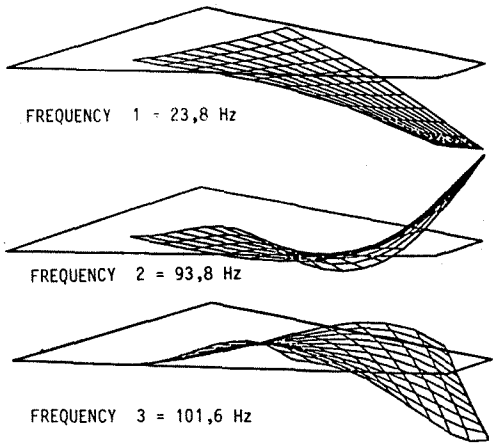

Fig. 12 Eigenmodes for increased pitch stiffness

Flutter Optimization with Structural Design Variables

If flutter speed is used as objective function and skin thickness coefficients and fiber orientations are design variables, it is possible to increase the flutter speed within a rather small range. But the optimization only works well within a band of high spigot pitch stiffners values. For $K_1 = 508 \frac{kNm}{rad}$, $K_2 = 734 \frac{kNm}{rad}$, and $K_3 = 175 \frac{kN}{m}$ the flutter speed can be increased from 1144 to 1300kts with an increase in weight of 7.4 lbs. In this case, the three layers are only allowed to rotate together. Fig. 13 depicts the general layer composition and fiber orientation for this design.

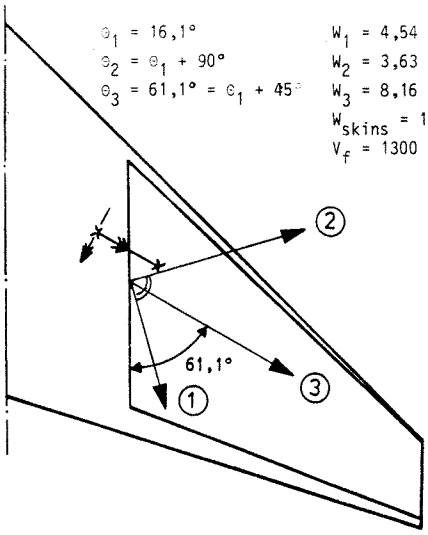

unbalanced, symmetric design

Fig. 13 Layer distributions for increased flutter speed

If the fiber angles can be rotated independently, the flutter speed is 1322 knots with only 4.1 lbs more compared to the initial design. Fig. 14 shows the thickness distributions, deformations, mode shapes and the flutter calculation for this design. In this case, the 0°-direction is swept back 5 degrees while in the first case the swept back 45°-direction has a higher amount of fibers to achieve the same result.

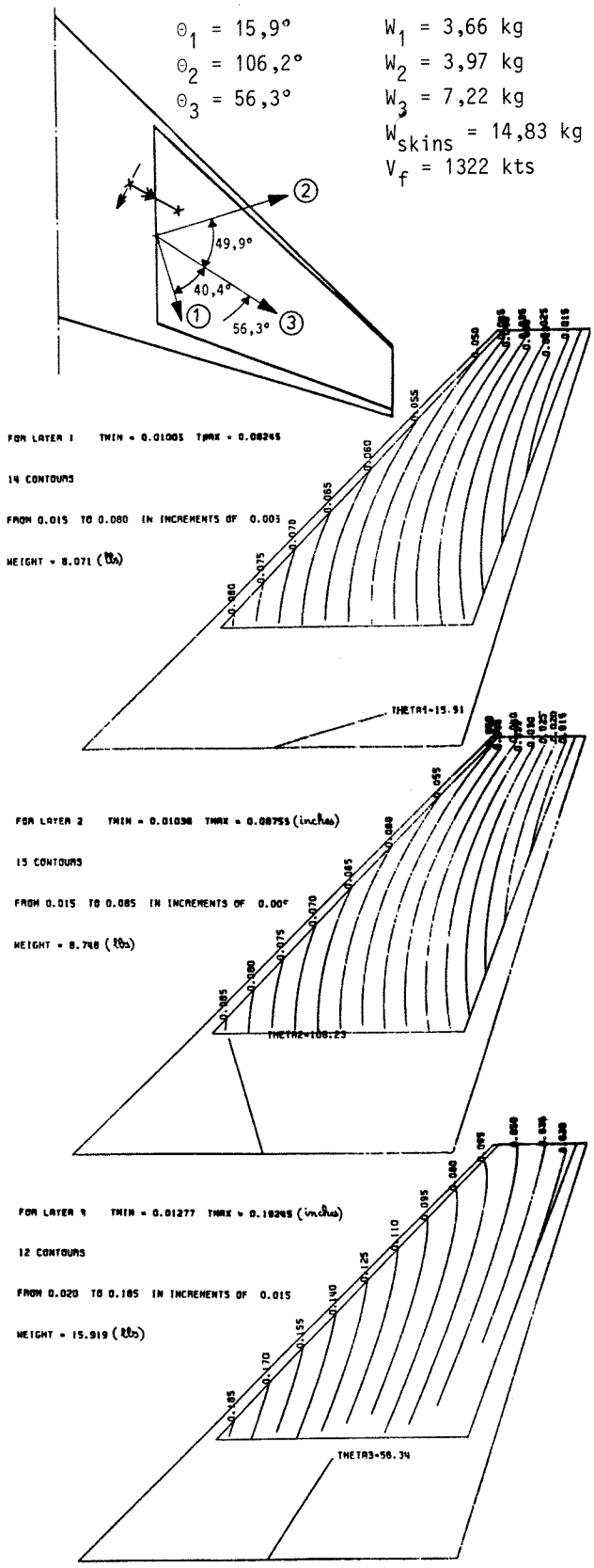

a) Thickness distributions

Fig. 14 Design with free fiber angles

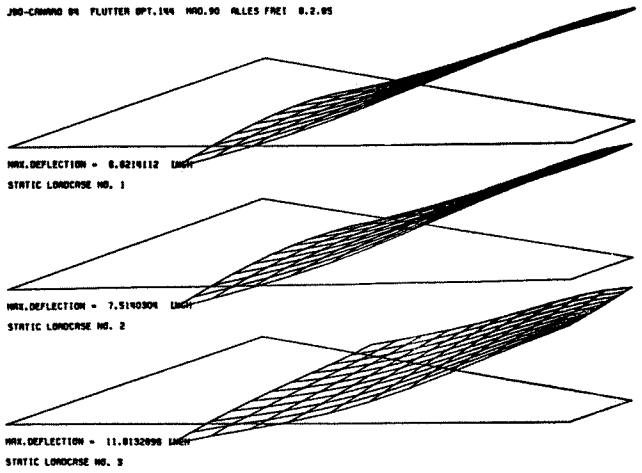

b) Static deflections

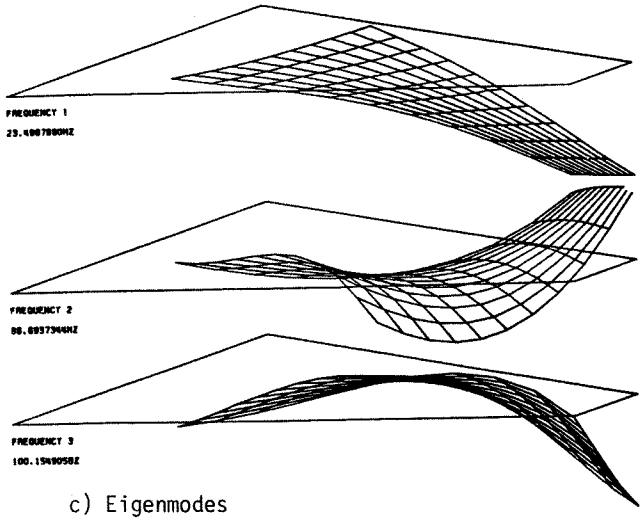

c) Eigenmodes

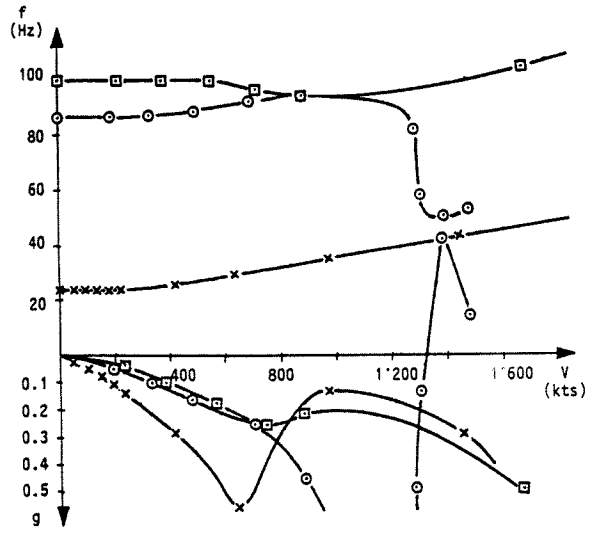

d) Flutter calculation

Fig. 14 Design with free fiber angles

To study the possibilities of flutter optimization in a free-floating mode, the attachment pitch stiffness was lowered. In fig. 15 the initial and final flutter speeds from the optimization are plotted versus pitch stiffness. For too small and too high values of K_2, the sensitivity of the structure to influence flutter is reducing. This can be explained for small pitch stiffness because rigid body pitch is dominant, and for high pitch stiffness the diagonal stiffness terms become dominant over the off-diagonal terms due to cross-coupling of the anisotropic material.

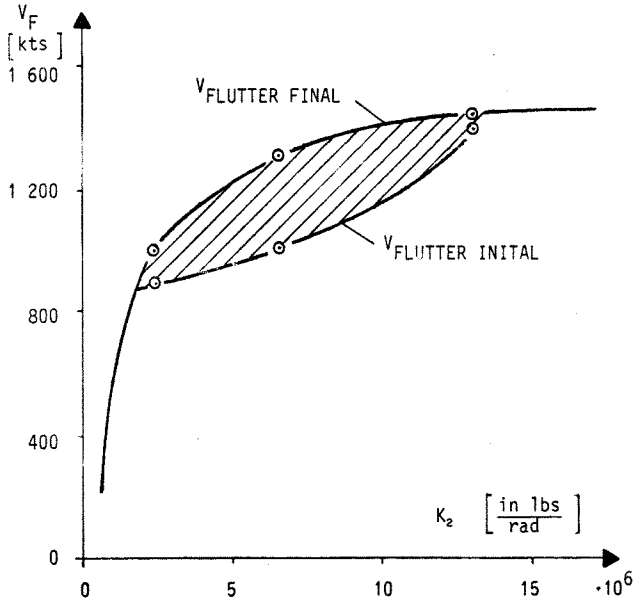

Fig. 15 Potential for optimization with different spigot pitch stiffness values

Optimization with Balance Masses

It was also tried to improve the flutter situation with balance masses. For this approach the 4 corner points on the surface, fig. 16 , were chosen for these masses. No improvement could be shown for the used range of attachment stiffnesses.

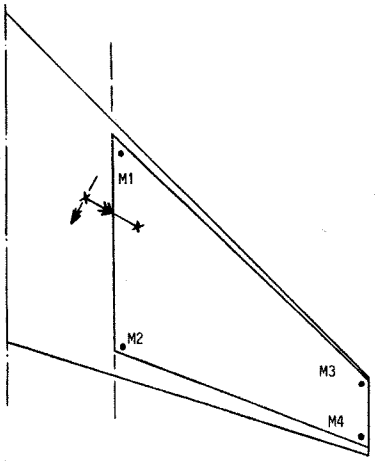

Fig. 16 Location of balance masses

Conclusions

Flutter is the most critical aeroelastic instability of a foreplane. The structural parameter that mainly controls this mechanism is the pitch stiffness of the spigot connecting the surface to the fuselage. Compared to this spring, the stiffness of the surfaces is already very high as a fallout from strength requirements. Therefore the potential of aeroelastic tailoring is rather limited. Another geometrical reason is the single point attachment predescribing the elastic deformations of the structure. The power of aeroelastic tailoring also increases with the area of a surface which is rather small in this case.

All efforts to find a flutter - free solution for a free-floating canard were unsuccessful.

References

/1/ Weisshaar T.A., Ryan R.J. : Control of Aeroelastic Instabilities Through Stiffness Cross-Conpling. Journal of Aircraft, Vol 23, No.2; New York, U.S.A., 1986.

/2/ Shirk M.H., Hertz T.J., Weisshaar T.A. : Aeroelastic Tailoring - Theory, Practice, and Promise. Journal of Aircraft, Vol 23, No. 1; New York, U.S.A., 1986.

/3/ Ponzi C. : Studio della dinamica strutturale di un velivolo supersonico in vista dell' applicazione del controlli attivi. Tesi di laurea, Facolta´di Ingegneria, Universitá di Roma, Italy, 1985

/4/ Aeroelastic Tailoring of Advanced Composite Structures for Military Aircraft, AFFDL-TR-76-100, Vol. I-III, Wright-Patterson AFB, Ohio, U.S.A., 1976

/5/ Krammer H., Schmid H., Hörnlein H.: Modifications for TSO. Internal MBB report, 1985.